Revealing the pure confinement effect in glass-forming liquids by dynamic mechanical analysis

J. Koppensteiner* and W. Schranz†
Faculty of Physics, University of Vienna, Boltzmanngasse 5, A-1090 Vienna, Austria

M. A. Carpenter
Department of Earth Sciences, University of Cambridge, Downing Street, Cambridge CB2 3EQ, United Kingdom
(Received 5 August 2009; revised manuscript received 15 October 2009; published 5 January 2010)

The dynamic mechanical response of mesoporous silica with coated inner surfaces confining the glass-forming liquid salol is measured as a function of temperature and frequency (1–100 Hz) for various pore sizes (2.4–7.3 nm). Compared to former results on natural pores, a distinct acceleration of dynamics due to the removal of surface-related retardation of molecular dynamics is found now, which can be fitted by a homogeneous relaxation using an unmodified Vogel-Fulcher-Tammann relation. This lubrication effect leads to a stronger decrease in the glass transition temperature T_g with decreasing pore size. The present data allow to quantify and separate competing side effects as surface bondings and negative pressure from the pure confinement induced acceleration of molecular dynamics with decreasing pore size. We analyze the dynamic elastic susceptibility data in terms of a recently proposed procedure [C. Dalle-Ferrier *et al.*, Phys. Rev. E **76**, 041510 (2007)], which relates the number $N_{corr,T}$ of molecules, whose dynamics is correlated with a local enthalpy fluctuation, to the three-point dynamic susceptibility χ_T. The observed increase of $N_{corr,T}$ with decreasing temperature strongly indicates that the size ξ of dynamic heterogeneities increases when approaching the glass transition.

DOI: 10.1103/PhysRevB.81.024202 PACS number(s): 64.70.P−, 61.20.Lc, 62.25.−g

I. INTRODUCTION

Glass-forming materials have been produced by mankind for more than 6000 years. Despite several decades of intense research the transition of a liquid into its glassy state is still lacking a universal theory explaining both the increase of viscosity η and molecular relaxation rates by 14 orders of magnitude[1,2] without creating any long-range order. A widely used explanation which goes back to Adam and Gibbs[3] is based on the assumption of cooperative rearrangement of molecules ("cooperative rearranging regions"), forming compact clusters of a typical size ξ. Such a subsystem of molecules can rearrange into another configuration independently of its environment.

The size of these groups of molecules is considered to grow to some nm as T_g is approached.[4] E.g., random first-order transition theory of glasses[5,6] predicts $\xi = r_0 0.51 (\ln \frac{\tau}{\tau_0})^{2/3}$. At T_g where $\tau \approx 100$ s one obtains for typical values of $\tau_0 \approx 10^{-12}$ s and $r_0 \approx 1$ nm, $\xi(T_g) \approx 5$ nm. Measuring such dynamic heterogeneities is one of the most important but at the same time difficult issues in the field of glass formation. Experimental setups such as specific-heat spectroscopy,[4,7] multidimensional NMR,[8–10] and dielectric spectroscopy,[11] have been used to determine a possible growing length scale accompanying the glass transition. All these results agree in the fact that the obtained cooperative regions are of the order of several nm near T_g and are displaying a weak temperature dependence.[12] Recent computer simulations also confirm a rather modest growth of the dynamically correlated regions when approaching the glass transition from above.[13] Very recently in a groundbreaking work Biroli *et al.*[14] found direct evidence for a growing dynamical length in supercooled liquids by applying inhomogeneous mode-coupling theory. Based on this theory these authors have recently developed a method to quantify the size of the correlated regions[11] by analyzing three-point dynamic susceptibilities. For a large number of supercooled liquids they could indeed confirm growing of the correlated regions when approaching the glass transition.[15]

However, direct measurements of ξ are extremely difficult, sometimes even impossible and one has to resort to indirect investigations. A widely used approach is confining the glass-forming liquid spatially, either in the form of thin films or by using mesoporous host matrices for confinement. If the size d of the confinement is finite the cooperatively rearranging regions cannot grow beyond any bound, becoming saturated at $\xi = d < \infty$. This should lead to a confinement induced acceleration of the dynamics resulting in a downshift of the glass transition, and even impeding it[16] as $\xi > d$.

Since the pioneer work of Jackson and McKenna[17] in 1991, uncovering a reduction of the glass transition temperature $\Delta T_g \propto 1/d$ in confinement of size d, a variety of confinement geometries and experimental methods have been used. Both weak and strong glass-forming liquids, showing strong and weak interaction with the two-dimensional or three-dimensional confinement media were investigated. Single, double, even multiple transitions have been observed. Extensive topical overviews are found in Refs. 18–20.

The abundance and diversity of experimental findings shows that an accurate discussion of side effects in discussing results of glass-forming liquids in confinement is essential. Negative pressure due to mismatching thermal-expansion coefficients of liquid and confining matrix is such a side effect. It was discussed by various authors[21,22] and sometimes even made responsible for the whole downshift of T_g in confinement.[21] Being true, it would disprove the idea of a growing length scale of cooperativity. In a former paper[23] the authors have determined negative pressure effects for salol in natural uncoated pores of size 7.5–2.6 nm from high-

TABLE I. N_2 adsorption characteristics and elastic moduli of untreated and silanated porous silica samples.

Untreated	Gelsil 2.6	Gelsil 5	Vycor
Av. pore diameter (nm)	2.6	5.0	7.5
Surface area (m^2/g)	590	510	70
Pore volume (cm^3/g)	0.38	0.68	0.21
Porosity ϕ	0.36	0.54	0.40
Bulk mod. K (GPa)	9.6	3.9	8.1
Shear mod. G (GPa)	7.7	3.3	6.7
Young´s mod. Y (GPa)	18.2	7.7	15.8
Silanated			
Av. pore diameter (nm)	2.4	4.8	7.3
Surface area (m^2/g)	260	325	65
Pore volume (cm^3/g)	0.15	0.4	0.19
Porosity ϕ	0.30	0.49	0.33
Bulk mod. K (GPa)	9.6	3.3	9.1
Shear mod. G (GPa)	9.0	3.9	9.0
Young´s mod. Y (GPa)	20.6	8.9	20.3

resolution thermal-expansion measurements. An upper bound for the contribution of negative pressure to the total downshift of T_g of $\approx 30\%$ was found.

A second and much larger effect on the glass transition of liquids in confinement arises from the interaction of the molecules with the huge inner surface of confining host matrices which can take values up to 600 m^2/g (see Table I). Confined liquids tend to form H bonds with the hydrophilic pore surface, which leads to an immobile surface layer of molecules and a retarded relaxation behavior when approaching the glass transition.

In recent dynamic elastic measurements[23,24] of salol filled into matrices of Vycor and Gelsil with natural untreated pores we studied this competition between surface induced slowing down and confinement induced acceleration of the dynamics. Here we present results of salol confined in mesoporous Vycor and Gelsil with silanated pore surfaces. The results clearly show that silanation removes the liquid-surface interaction to a large extend, leading to an enhancement of the molecular dynamics in the pores, resulting in a stronger downshift of T_g as compared to the uncoated pores. These findings allow to separate the surface effect from confinement induced acceleration, and a simultaneous quantitative statement about negative pressure (no change due to silanation) within one and the same measurement technique and confinement geometry. A comparison with previous dielectric spectroscopy data[25–27] of salol in mesoporous matrices yields excellent agreement. Using the recently proposed method of Berthier *et al.*[11] we determine the number $N_{corr,T}$ of dynamically correlated molecules as a function of temperature and pore size.

II. EXPERIMENTAL

A. Sample preparation

Vycor by Corning Inc., New York, is produced via phase separation within a Na_2O-B_2O_3-SiO_2 melt, and subsequent acid leaching,[28] which leaves a 98% pure SiO_2 skeleton containing interconnected pores of random length, direction and density. A very narrow pore size distribution and an average ratio of pore length l over pore diameter d of $l/d \approx 4.35$ is reported.[29] Gelsil samples result from a sol-gel process[30] and consist of randomly formed pure fused SiO_2 monodisperse spheres,[31] touching and penetrating each other, resulting in a mesoporous structure with a rather broad distribution of pore diameters, as N_2-sorption results showed. Samples are cut and sanded to gain the required orthogonal shapes, and cleaned in a 30% H_2O_2 solution at 363 K for 24 h. Drying is done under high vacuum (10^{-6} mbar) at 393 K for another 24 h.

In order to deactivate inner surfaces, OH^- groups are replaced by $OSi(CH_3)_3$ trimethylsilyl groups via exposing cleaned samples to gaseous hexamethyldisilazane (HMDS, from Sigma Aldrich, purity 99.9%) in a closed vessel at 330 K for 24 h. Afterwards samples are again evacuated for 24 h at 300 K. In order to check pore geometry and pore radius after silanation, mesoporous samples have been tested via N_2-sorption and BET/BJH analysis of the individual desorption isotherms[32] experiments before and after HMDS treatment (Table I). The samples surface area, pore volume and porosity were found to decrease due to silanation. The effect of silanation on the pore diameter is ≈ 0.2 nm, corresponding to a HMDS layer thickness of ≈ 0.1 nm. For comparison Kremer *et al.*[25] estimated the thickness of the silan layer from analysis of dielectric strength data as 0.38 nm.

Filling with the fragile low molecular weight glass former[33] phenylsalicylate (salol, $C_{13}H_{10}O_3$, $T_m^{bulk}=316$ K) is done by capillary wetting at 333 K for 12 h. Filling fractions f are evaluated via weighing clean and filled samples. Vycor pore space can usually be filled up completely ($f \approx 1$), whereas for Gelsil samples $f \approx 0.9$ is usually achieved due to blocking of bottleneck-shaped pores and closed pores which cannot be reached by the liquid.

Some characterizing parameters for the glass-freezing behavior of bulk salol are: fragility index m—which usually varies from $m=17$ for strong glass formers to $m=150$ for fragile ones—takes for salol[34] the value $m=73$, $T_g^{bulk}=220$ K (glass transition temperature defined at $\tau=100$ s) and $T_0=175$ K (Ref. 35) (bulk Vogel-Fulcher temperature). The volume of a salol molecule is estimated[36] as 0.282 nm^3 corresponding to a mean diameter of about 0.8 nm.

B. Dynamic mechanical analysis

The dynamic mechanical response of samples of a typical size of $1 \times 2 \times 8$ mm^3 in three-point bending mode yields the real and imaginary part of the complex Young's modulus $Y^*=Y'+iY''$ within a frequency range of 0.01 to 100 Hz applying static and dynamic forces up to 9.8 N. For further details see Refs. 23, 24, 37, and 38. Temperature is controlled by gaseous nitrogen flow from 120 K to room temperature. Dynamic mechanical analyzers (DMAs) are decoupled from building vibrations, and electronics are shielded from a possible interference with the 50 Hz mains voltage frequency. The analyzers used are a series 7 DMA and a diamond DMA, both built by Perkin Elmer Inc.

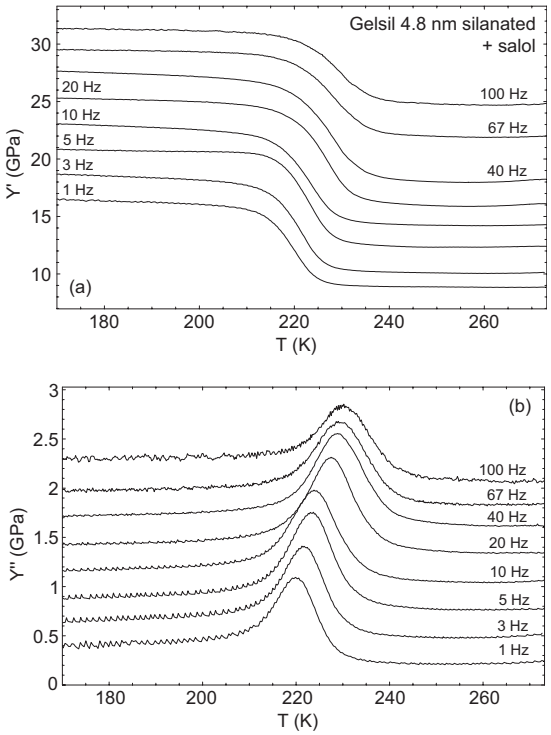

FIG. 1. (a) Real (b) and imaginary parts of the complex Young´s modulus of silanated Gelsil (4.8 nm) filled with salol (filling fraction $f=0.87$) measured in three-point bending geometry (diamond DMA). 1 Hz signal are original data, other signals are offset for sake of clarity since there is no frequency dependence of low and high-temperature values aside the glass transition.

C. Resonant ultrasound spectroscopy

Due to contact errors a DMA experiment does not yield absolute values for elastic moduli. Therefore resonant ultrasound spectroscopy (RUS) was used to determine bulk and shear moduli of both natural and silanated mesoporous samples at room temperature. Orthogonal parallelepipeds of about $2.9\times3.0\times3.1$ mm^3 were used to gather resonance spectra from 50 to 1100 kHz. For each sample 25 peaks resulting from excited resonant eigenmodes and corresponding overtones then were fitted via a Lagrangian minimization routine gaining bulk modulus K and shear modulus G (see Table I) with an accuracy of less than 1%. For further experimental details see, e.g., Ref. 39. Young´s modulus Y was calculated from $Y=9KG/(3K+G)$ and used to calibrate DMA raw data at room temperature (see Figs. 1–3).

III. RESULTS AND DISCUSSION

As an example, the dynamic elastic response (1 Hz–100 Hz) of salol in Gelsil with silanated pores of 4.8 nm diameter is shown in Fig. 1. The data for 2.4 and 7.5 nm pores look very similar and are hence not presented here.

Figure 2 gives a comparison between the recent results of salol in natural untreated pores[23] and the data on silanated samples. The most striking feature of the silanated samples is the absence of a double-peak structure in $Y''(T)$ and the steplike shape in $Y'(T)$. In untreated samples a significant part of the confined liquid sticks to the pore surface due to hydrogen bonding, thus being retarded in relaxation dynamics. This leads to a local dependence of relaxation times across the pore section (see Fig. 4) causing an extra glass transition at higher temperature relative to the one of the core molecules. Assuming a spatial distribution of Vogel-Fulcher temperatures[40] $T_0(r)=T_{00}+k/(R-r+r_p)$, which translates via $\tau(r)=\tau_0\cdot\exp\{E/[T-T_0(r)]\}$ to a distribution of relaxation times we were able to fit the stepwise change in $Y'(T)$ and the double-peak structure in $Y''(T)$. A detailed analysis can be found in Ref. 23.

For silanated surfaces we now find only bulklike relaxation, i.e., just one step in $Y'(T)$ and one single narrow peak in $Y''(T)$. Peaks do shift with measurement frequency, as Fig. 1 shows. Since the liquid-surface interaction is removed now, we do not take into account any radial dependence of the relaxation time (see Fig. 4), but use a single homogeneous Vogel-Fulcher-Tammann equation

$$\tau(T,d)=\tau_0\cdot\exp\left[\frac{E}{T-T_0(d)}\right] \tag{1}$$

with the pre-exponential factor τ_0, the activation energy E and the Vogel-Fulcher temperature $T_0(d)$, which depends on the pore diameter d.

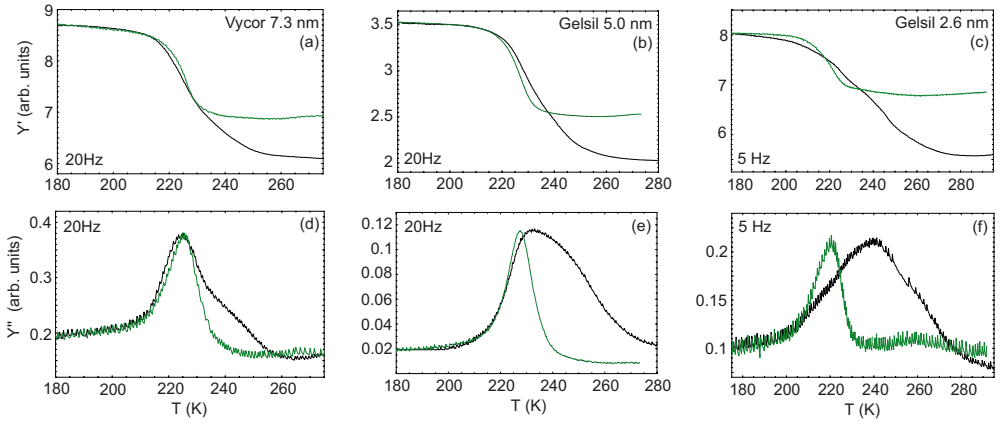

FIG. 2. (Color online) Comparison of DMA data: black lines represent untreated samples; green (gray) lines are data for silanated pore surface. Since contact losses inhibit direct comparison, Y' and Y'' signals of silanated samples were scaled i.o. to match Y'' peak heights.

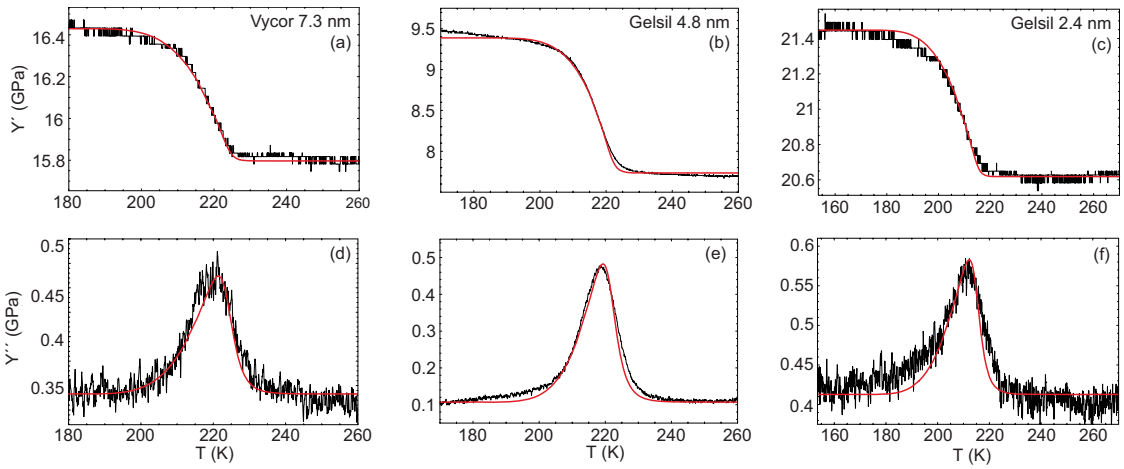

FIG. 3. (Color online) Real part Y' and imaginary part Y'' of different porous samples filled with salol, calibrated using RUS results at room temperature. Lines are fits using Eqs. (1), (3a), and (3b) with parameters of Table II.

Similar as in our previous work[23,24] a Cole-Davidson relaxation is used to model dynamic mechanic susceptibility in terms of (now radially monodisperse) relaxors

$$Y^*(\omega) \propto \frac{1}{(1+i\omega\tau)^{\gamma}} \tag{2}$$

with $\omega=2\pi\nu$, ν being the measurement frequency, and the broadening parameter[41] γ. Separating real and imaginary part of $Y^*=Y'+iY''$ leads to

$$Y'(T,d) = 1 - \Delta Y \frac{\cos\{\gamma \cdot \arctan[\omega\tau(T,d)]\}}{[1+\omega^2\tau(T,d)^2]^{\gamma/2}} \tag{3a}$$

$$Y''(T,d) = \Delta Y \frac{\sin\{\gamma \cdot \arctan[\omega\tau(T,d)]\}}{[1+\omega^2\tau(T,d)^2]^{\gamma/2}}. \tag{3b}$$

Equations (1), (3a), and (3b) are used to fit the data given in Figs. 1 and 2. We point out that T_0 enters as a fit parameter depending on the pore size d. Fits and corresponding parameters are shown in Fig. 3 and Table II, respectively.

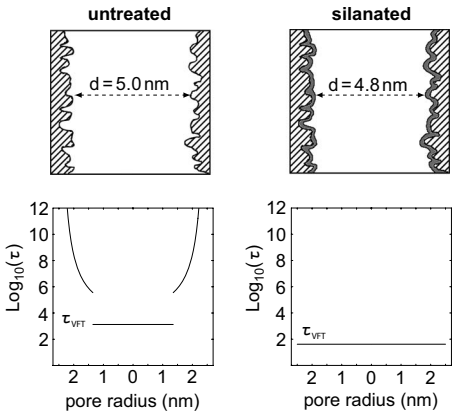

FIG. 4. Modeled relaxation time in untreated and silanated pores of Gelsil 5 from Eq. (1) used in Ref. 23 and in Eqs. (3a) and (3b) for fits of data in Figs. 3(b) and 3(e) herein, at $T=220$ K.

Silanation causes two main effects on the dynamics of the molecules within the pores:

(1) For untreated surface, we had to consider pore center relaxation times about two orders of magnitude higher[23] than obtained from the present analysis of silanated pores. Such an enhancement of mobility of molecules due to the absence of surface blocking in silanated pores was also observed in previous studies.[27,42] It probably reflects the fact that the surface blocking of molecular mobility in uncoated pores slows down the dynamics of molecules also in the center of the pores.

(2) Present results and used fit parameters (Table II) show that the acceleration of the dynamics in silanated pores now leads to a much stronger downshift of T_g with decreasing pore size as compared with the results of uncoated pores.[23] It reflects the pure confinement effect—i.e., free of surface contributions—which leads to a downshift of T_g due to limitation of the correlated regions by the pore diameter (Fig. 6).

On the other hand, silanation does not seem to have an effect on negative pressure within pores: Thermal-expansion experiments using silanated samples were performed as already done for untreated samples in Ref. 23. The result for Gelsil 5.0 nm is displayed in Fig. 7. Whereas silanated samples show less adsorption swelling probably due to a reduced surface tension [see Eq. (6) of Ref. 23], the temperature T^* at which thermal contraction again balances swelling and no pressure is applied upon the liquid, is not changed by silanation. This is possible due to a less steep contraction and smaller thermal-expansion coefficient of the filled silanated sample. The calculated negative pressure induced downshift

TABLE II. Fit parameters used in Eqs. (3a) and (3) for fits of Fig. 3.

	Vycor	Gelsil5	Gelsil2.6
E (K)	1750	1750	1750
T_0 (K)	161.5	158.5	154.5
τ_0 (s)	10^{-13}	10^{-13}	10^{-13}
γ	0.19	0.25	0.17

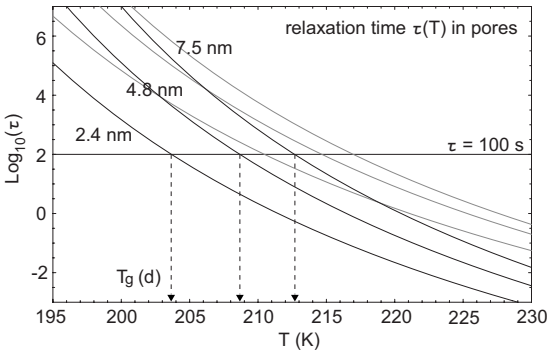

FIG. 5. Relaxation time in pore centers calculated from Eq. (1) with corresponding parameters from Table II. Horizontal line shows $\tau=100$ s. Gray lines are relaxation times in untreated pores from Ref. 23.

ΔT_g following the procedure of Sec. IIIC of Ref. 23 is −2.6 K compared to −2.4 K deduced for untreated pores. Also for silanated Vycor we found the same negative pressure contribution as compared to untreated Vycor. Thus, the enhancement of the size effect of $\Delta T_g(d)$ in coated pores results from the reduction of the chemical bonding of the glass-forming liquid with the pore surface due to silanation.

Unfortunately there is no unique theory which clearly relates these finite-size effects to parameters characterizing the glass transition. However in recent computer simulations[43] of supercooled polymer films confined between two separated walls of distance d it was shown that confinement leads to faster dynamics. The authors parametrized the size dependence of the relaxation time as $\tau(T,d)\propto\exp[\frac{E(d)}{T-T_0(d)}]$ and found similar d dependencies for the mode-coupling critical temperature $T_c(d)$ and the Vogel-Fulcher temperature $T_0(d)$ arguing, that $T_g(d)$ should also follow a similar curve (see Fig. 14 of Ref. 43). As already mentioned above we here use the same dependence of the relaxation time [Eq. (1)] to fit our data and obtain a very similar size dependence of $T_g(d)$ and $T_0(d)$ (Fig. 8) as Varnik *et al.*

Hunt[44] calculated finite-size effects on the glass transition temperature in glass-forming liquids analytically using percolation theory. Assuming a Gaussian distribution of barrier heights $n(E)\propto\exp[(E-E_m)^2/2\sigma^2]$ with $E_m\approx\sigma$ [Eq. (6) of Ref. 44] it was found that

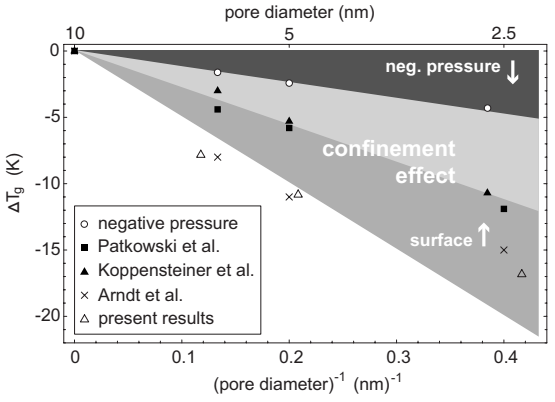

FIG. 6. Shift of glass transition temperature against inverse pore diameter. Open circles display the maximum negative pressure contribution (see Sec. IIIC of Ref. 23); boxes are ΔT_g's Ref. 23, filled triangles show literature values from Ref. 21. Open triangles are the present results, and crosses mark corresponding literature data from Ref. 25.

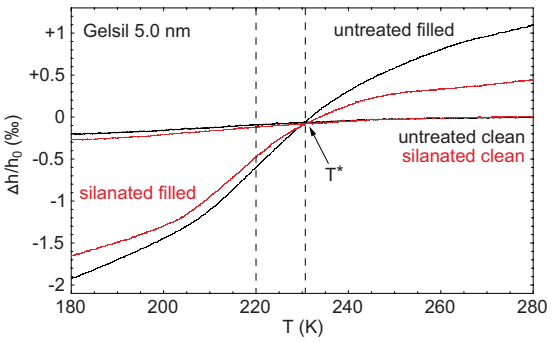

FIG. 7. (Color online) Linear thermal expansion of untreated (black) and silanated (red/gray) Gelsil 5.0 nm, both empty and filled. Sample height is normalized at 280 K.

$$T_g^{bulk}=\frac{1.75\sigma}{k_B\ln(t/\tau_0)}, \tag{4}$$

where t defines the laboratory time scale ≈100 s of the glass transition. For the confinement induced shift of the glass transition temperature, the author obtained

$$T_g(d)=T_g^{bulk}\left[1-\frac{0.5\sigma}{k_B\ln\left(\frac{100}{\tau_0}T_g^{bulk}\right)}\frac{r_0}{d}\right], \tag{5}$$

where r_0 is the typical distance between molecules, which we approximate here as the diameter of a salol molecule $r_0\approx0.8$ nm. Inserting Eq. (4) into Eq. (5) yields

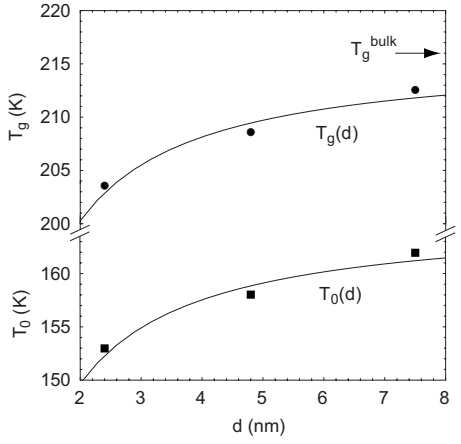

FIG. 8. Shift in glass transition temperature T_g and Vogel-Fulcher temperature T_0 against pore diameter d. The points are determined from fitting the experimental data with Eqs. (1), (3a), and (3b), where $T_g(d)$ is obtained from $\tau(T,d)=100$ s, as shown in Fig. 5. The lines are fits using Eq. (6) yielding $c=0.13$ and $T_g^{bulk}=216$ K. For calculating $T_0(d)$ the relation $T_g-T_0=\frac{E_g}{\ln(100/\tau_0)}=50.6$ K was used, as indicated in the text.

$$T_g(d) = T_g^{bulk}\left[1 - c\frac{r_0}{d}\right], \tag{6}$$

where $c=0.286$. Given the semiquantitative character of this theory, the agreement with our determined value of $c=0.13$ is quite reasonable. In this picture T_g is reduced by confinement because the average barrier height for the molecules in pores is smaller than the so-called "blocking" barrier, which is responsible for the glass freezing in the bulk. We have also plotted the values of $T_0(d)$ of Table II in Fig. 8. The corresponding line was drawn using the relation $T_g - T_0 = \frac{E}{\ln(100/\tau_0)} = 50.6$ K, which is obtained from Eq. (1) using the fit parameters $E=1750$ K and $\tau_0 = 10^{-13}$ s of Table II.

As already mentioned above, Dalle-Ferrier *et al.*[15] gave an expression for the number $N_{corr,T}$ of molecules that are dynamically correlated with local enthalpy fluctuations over a time interval of the order of τ as

$$N_{corr,T}(T) = \frac{T}{\sqrt{\Delta C_p}}(\max_\omega|\chi_T(T,\omega)|), \tag{7}$$

where $\chi_T(T,\omega) := \frac{\partial\chi(T,\omega)}{\partial T}$, $\chi(T,\omega)$ is a normalized suitable dynamic correlation function and ΔC_P in units of the gas constant R is the excess specific heat of the glass-forming liquid at constant pressure.[15] Very often glass-forming materials are studied by dielectric spectroscopy measurements and therefore the dynamic susceptibility is identified with the dielectric susceptibility. To estimate $N_{corr,T}$, we apply two different procedures: In the first one we are using $\chi(T,\omega) := \frac{Y'(\omega)-Y'(\infty)}{Y'(0)-Y'(\infty)}$ in Eq. (7) to analyze the data directly, i.e., without any fit procedure in between. In the second case we rewrite Eq. (7) with Eq. (2) yielding

$$N_{corr,T}(T) = \frac{T}{\sqrt{\Delta C_p}} f(\gamma)\left(\frac{\partial \ln \tau}{\partial T}\right), \tag{8}$$

where $\tau(T)$ is obtained from fits of the data in Fig. 3 and $f(\gamma) = \frac{\sin[\gamma \arctan(\frac{1}{\gamma})] + \frac{1}{\gamma}\cos[\gamma \arctan(\frac{1}{\gamma})]}{(1+\gamma^{-2})^{1+\gamma/2}}$ results from the Cole-Davidson dynamic response function and is the analog to the stretched exponential β of the KWW-response function used, e.g., in Eq. (8) of Ref. 45. It should be noted that Eq. (8) is only strictly valid, if γ is independent of temperature (see discussion in Ref. 15). Figure 9 compares the temperature dependence of $N_{corr,T}$ calculated from the two different methods, which results in excellent agreement in the temperature range $220 < T < 235$ K. This implies that at least in this temperature range γ is temperature independent.

Although it is not straightforward, it is tempting to estimate the size of ξ of dynamic heterogeneities for the present case i.o. to compare it with values determined from other types of experiments. As shown e.g., in Refs. 11 and 15 the height of the peak in the nonlinear susceptibility χ_4 yields the correlation volume, i.e., $\chi_4 \approx (\frac{\xi}{a})^\zeta$, where $2 < \zeta < 4$ (Ref. 46) and a is the molecular size, i.e., 0.8 nm for salol. Quite generally $\chi_4 \geq \frac{T^2}{\Delta C_p}\chi_T^2$. However, for most fragile liquids the equality $\chi_4 \approx \frac{1}{\Delta C_p}T^2\chi_T^2$ can be assumed.[11,15]

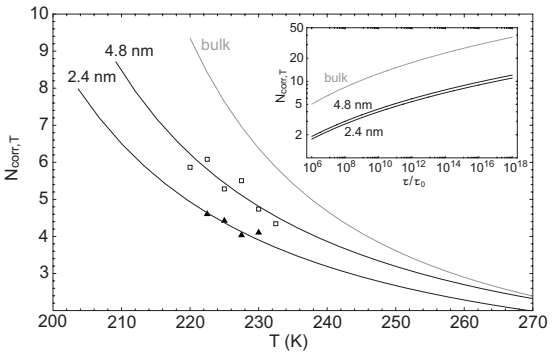

FIG. 9. Temperature dependence of $N_{corr,T}$ for various pore sizes. Lines are calculated from Eq. (8) using the procedure described in the text. Symbols are calculated from DMA data using Eq. (7). Inset shows $N_{corr,T}$ against relaxation time τ/τ_0 in the corresponding temperature range on logarithmic scales.

Assuming a compact correlation volume, i.e., $\zeta=3$, we can estimate $\xi = (N_{corr,T}^2)^{1/3}a$ yielding a growth of ξ from about 1.6 nm at $T=270$ K to 3.2 nm at $T_g(d)$ which is nearly the same value for any measured pore size d. Although there are uncertainties about numerical prefactors,[15] as well as the geometry for heterogeneities, i.e., the exponent ζ, the overall behavior of $\xi(T_g,d)$ is in remarkable agreement with calorimetrically determined characteristic lengths for salol in confined geometries,[47] as well as with dielectric measurements.[48]

IV. CONCLUSIONS

Results of extensive dynamic mechanical measurements of the glass-forming liquid salol confined in mesoporous silica with silanated pores are presented. It turns out that silanation is able to reduce the liquid-surface interactions drastically. At the same time high-resolution thermal-expansion measurements show that the negative pressure contribution to the downshift of the glass transition temperature T_g is the same as in uncoated pores. As a result the observed stronger (as compared to uncoated pores) downshift of T_g with decreasing pore size can be fully attributed to the confinement induced acceleration of the dynamics, which occurs due to the hindering of cooperativity. Using the results of percolation theory[44] we have calculated the downshift of T_g with decreasing pore size, which fits our data very well. In Ref. 44 it is also shown that finite-size effects are expected to set in when the pore size $d \approx 7r_0 - 10r_0$ yielding 4.8–8 nm for salol with $r_0 \approx 0.8$ nm. This is in very good agreement with our observations.

We also have analyzed our dynamic elastic data obtained for the different pore sizes in terms of a proposed theory[11] which relates the number of dynamically correlated molecules $N_{corr,T}$ to the temperature derivative of the dynamical two-point correlation function, which in our case can be identified with the dynamic elastic susceptibility $Y(\omega,T)$. The results clearly show an increase of $N_{corr,T}$ with decreasing temperature approaching T_g. In spite of the fact that the precise relation between $N_{corr,T}$ and a corresponding length scale is hampered due to unknown prefactors and

exponents,[15] this implies that the pore size ξ of dynamically correlated regions increases when approaching T_g.

For smaller pore sizes $\xi(T',d)$ at a given temperature T' shifts to smaller values which is concomitant to the systematic decrease of the relaxation time $\tau(T',d)$ and the resulting downshift of $T_g(d)$. However at the glass transition temperature the dynamic correlation length is almost independent of the pore size with $\xi(T_g,d)=3.2$ nm, a value which was also found by calorimetric[47] and dielectric[48] measurements.

Very similar as already observed in Ref. 15, we found a modest growth of $N_{corr,T}$ from about 2 at $T=270$ K to 8 at T_g, whereas the relaxation time τ increases dramatically by about 12 orders of magnitude in this temperature interval (see inset of Fig. 9). This characteristic behavior was observed for all measured pore sizes.

Unfortunately at present there is no unique theory that relates the relevant parameters controlling the confinement effects in glass-forming materials to experimental data. The reason for this is that the microscopic mechanism behind the glass transition is still not completely understood and more theoretical (e.g., of the type presented in Ref. 49) and experimental work is required to close the gap of knowledge and understand confinement effects in glass-forming liquids.

ACKNOWLEDGMENTS

We thank Marie-Alexandra Neouze and the Institute of Materials Chemistry from the Vienna University of Technology for the N_2 characterization of our samples. We also thank Irena Drevenšek-Olenik and Miha Devetak from the Jožef-Stefan-Institute in Ljubljana for help concerning silanation, which was done within ÖAD-WTZ Project No. Sl 19/2009. RUS facilities in Cambridge were established with the support of grant to MAC from the Natural Environment Research Council of Great Britain, Grant No. NE/B505738/1. Support by the Austrian FWF (Grant No. P19284-N20) and by the University of Vienna within the IC Experimental Materials Science ("Bulk Nanostructured Materials") is gratefully acknowledged.

*johannes.koppensteiner@univie.ac.at
†wilfried.schranz@univie.ac.at

[1] M. Cukierman, J. W. Lane, and D. R. Uhlmann, J. Chem. Phys. **59**, 3639 (1973).
[2] M. D. Ediger, C. A. Angell, and S. R. Nagel, J. Phys. Chem. **100**, 13200 (1996).
[3] G. Adam and J. H. Gibbs, J. Chem. Phys. **43**, 139 (1965).
[4] E. Hempel, G. Hempel, A. Hensel, C. Schick, and E. Donth, J. Phys. Chem. B **104**, 2460 (2000).
[5] T. R. Kirkpatrick and P. G. Wolynes, Phys. Rev. A **35**, 3072 (1987).
[6] V. Lubchenko and P. G. Wolynes, Phys. Rev. Lett. **87**, 195901 (2001).
[7] E. Donth, H. Huth, and M. Beiner, J. Phys.: Condens. Matter **13**, L451 (2001).
[8] U. Tracht, M. Wilhelm, A. Heuer, H. Feng, K. Schmidt-Rohr, and H. W. Spiess, Phys. Rev. Lett. **81**, 2727 (1998).
[9] S. A. Reinsberg, A. Heuer, B. Doliwa, H. Zimmermann, and H. W. Spiess, J. Non-Cryst. Solids **307-310**, 208 (2002).
[10] X. H. Qiu and M. D. Edinger, J. Phys. Chem. B **107**, 459 (2003).
[11] L. Berthier, G. Biroli, J.-P. Bouchard, L. Cipelletti, D. El Masri, D. L'Hote, F. Ladieu, and M. Pierno, Science **310**, 1797 (2005).
[12] B. M. Erwin and R. H. Colby, J. Non-Cryst. Solids **307-310**, 225 (2002).
[13] P. Scheidler, W. Kob, K. Binder, and G. Parisi, Philos. Mag. B **82**, 283 (2002).
[14] G. Biroli, J.-P. Bouchaud, K. Miyazaki, and D. R. Reichman, Phys. Rev. Lett. **97**, 195701 (2006).
[15] C. Dalle-Ferrier, C. Thibierge, C. Alba-Simionesco, L. Berthier, G. Biroli, J. P. Bouchaud, F. Ladieu, D. L'Hote, and G. Tarjus, Phys. Rev. E **76**, 041510 (2007).
[16] A. Schönhals, H. Göring, C. Schick, B. Frick, and R. Zorn, Colloid Polym. Sci. **282**, 882 (2004).
[17] C. L. Jackson and G. B. McKenna, J. Non-Cryst. Solids **131-133**, 221 (1991).
[18] M. Alcoutlabi and G. B. McKenna, J. Phys.: Condens. Matter **17**, R461 (2005).
[19] C. Alba-Simionesco, B. Coasne, G. Dosseh, G. Dudziak, K. E. Gubbins, R. Radhakrishnan, and M. Sliwinska-Bartkowiak, J. Phys.: Condens. Matter **18**, R15 (2006).
[20] R. Kremer, A. Huwe, A. Schönhals, and A. S. Rzanski, *Molecular Dynamics in Confining Space in Broadband Dielectric Spectroscopy*, edited by F. Kremer and A. Schönhals (Springer Verlag, Berlin, 2000) p. 171.
[21] A. Patkowski, T. Ruths, and E. W. Fischer, Phys. Rev. E **67**, 021501 (2003).
[22] S. L. Simon, J.-Y. Park, and G. B. McKenna, Eur. Phys. J. E **8**, 209 (2002).
[23] J. Koppensteiner, W. Schranz, and M. R. Puica, Phys. Rev. B **78**, 054203 (2008).
[24] W. Schranz, M. R. Puica, J. Koppensteiner, H. Kabelka, and A. V. Kityk, EPL **79**, 36003 (2007).
[25] M. Arndt, R. Stannarius, H. Groothues, E. Hempel, and F. Kremer, Phys. Rev. Lett. **79**, 2077 (1997).
[26] M. Arndt, R. Stannarius, W. Gorbatschow, and F. Kremer, Phys. Rev. E **54**, 5377 (1996).
[27] F. Rittig, A. Huwe, G. Fleischer, J. Kärger, and F. Kremer, Phys. Chem. Chem. Phys. **1**, 519 (1999).
[28] T. H. Elmer, *Engineered Materials Handbook* (ASM International, Materials Park, OH, 1992) Vol. 4, p. 427.
[29] P. Levitz, G. Ehret, S. K. Sinha, and J. M. Drake, J. Chem. Phys. **95**, 6151 (1991).
[30] J.-L. R. Nogues and W. Moreshead, J. Non-Cryst. Solids **121**, 136 (1990).
[31] N. Eschricht, E. Hoinkis, F. Mädler, and P. Schubert-Bischoff, Stud. Surf. Sci. Catal. **144**, 355 (2002).
[32] F. Rouguerol, J. Rouguerol, and K. Sing, *Adsorption by Powders and Porous solids: Principles, Methodology and Applications* (Academic Press, New York, 1999).
[33] O. Trofymluk, A. A. Levchenko, and A. Navrotsky, J. Chem.

Phys. **123**, 194509 (2005).
[34] T. Scopigno, G. Ruocco, F. Sette, and G. Monaco, Science **302**, 849 (2003).
[35] R. Richert and C. A. Angell, J. Chem. Phys. **108**, 9016 (1998).
[36] E. Eckstein, J. Qian, R. Hentschke, T. Thurn-Albrecht, W. Steffen, and E. W. Fischer, J. Chem. Phys. **113**, 4751 (2000).
[37] W. Schranz, Phase Transitions **64**, 103 (1997).
[38] W. Schranz and D. Havlik, Phys. Rev. Lett. **73**, 2575 (1994).
[39] A. Migliori and J. D. Maynard, Rev. Sci. Instrum. **76**, 121301 (2005).
[40] R. Zorn, L. Hartmann, B. Frick, D. Richter, and F. Kremer, J. Non-Cryst. Solids **307-310**, 547 (2002).
[41] Note that by mistake Eq. (4) of Ref. 23 contains the exponent $\gamma/2$ instead of γ.
[42] G. Dosseh, C. Le Quellec, N. Brodie-Lindner, C. Alba-Simionesco, W. Haeussler, and P. Levitz, J. Non.-Cryst. Solids **352**, 4964 (2006).
[43] F. Varnik, J. Baschnagel, and K. Binder, Eur. Phys. J. E **8**, 175 (2002).
[44] A. Hunt, Solid State Commun. **90**, 527 (1994).
[45] S. Capaccioli, G. Ruocco, and F. Zamponi, J. Phys. Chem. B **112**, 10652 (2008).
[46] G. Biroli and J. P. Bouchaud, Europhys. Lett. **67**, 21 (2004).
[47] E. Donth, E. Hempel, and C. Schick, J. Phys.: Condens. Matter **12**, L281 (2000).
[48] F. Strichel, Ph.D. thesis, Mainz University, Germany, 1995.
[49] V. Krakoviack, Phys. Rev. Lett. **94**, 065703 (2005).